Supporting Information (SI Appendix)

Histone methylation-mediated microRNA-32-5p downregulation in sensory neurons regulates pain behaviors via targeting Cav3.2 channels

Renfei Qi [a], Junping Cao [a, e], Yufang Sun [a, f], Yanping Li [a], Zitong Huang [a], Dongsheng Jiang [b], Xing-Hong Jiang [a], Terrance P. Snutch [c], Yuan Zhang [d], Jin Tao [a, f]

[a] Department of Physiology and Neurobiology & Centre for Ion Channelopathy, Medical College of Soochow University, Suzhou 215123, P.R. China;

[b] Institute of Regenerative Biology and Medicine, Helmholtz Zentrum München, Munich 81377, Germany;

[c] Michael Smith Laboratories and Djavad Mowafaghian Centre for Brain Health, University of British Columbia, Vancouver, BC, V6T 1Z4, Canada;

[d] Department of Geriatrics & Clinical Research Center of Neurological Disease, the Second Affiliated Hospital of Soochow University, Suzhou 215004, P.R. China;

[e] Jiangsu Province Key Laboratory of Anesthesiology, Xuzhou Medical University, Xuzhou 221004, P.R. China;

[f] Jiangsu Key Laboratory of Neuropsychiatric Diseases, Soochow University, Suzhou 215123, P.R. China

Address correspondence to:

Dr. Jin Tao, Department of Physiology and Neurobiology & Centre for Ion Channelopathy, Medical College of Soochow University, 199 Ren-Ai Road, Suzhou 215123, P.R. China. E-mail: taoj@suda.edu.cn or Dr. Yuan Zhang, Department of Geriatrics & Clinical Research Center of Neurological Disease, the Second Affiliated Hospital of Soochow University, 1055 San-Xiang Road, Suzhou 215004, P.R. China. E-mail: yuanzhang@suda.edu.cn

This PDF file includes:

SI Materials and Methods

SI References

SI Figures S1 to S16

SI Materials and Methods

Animal model

All experimental procedures performed in this study were carried out in accordance with National Institutes of Health (NIH) guidelines and had been approved by the Institutional Animal Care and Use Committee of Soochow University. Every effort was made to minimize the number of animals used and animal suffering. Animals (Sprague-Dawley rats, 140-160 g, male) were housed (three to four rats per cage with soft bedding) under a standard 12/12-h light–dark cycle in a temperature- and humidity-controlled room with food and water provided *ad libitum*. A trigeminal neuropathic pain model was produced by chronic constriction injury to the left infraorbital nerve (CCI-ION) via an intraoral approach as described in previous studies (1-3) with some modifications. Briefly, after anesthetization with isoflurane, an approximately 1 cm incision was made along the gingivobuccal margin in the buccal mucosa of the rats beginning from the first molar. The left ION was dissected near the infraorbital foramen using glass rods. Two sutures (4-0 silk) were made loosely around the ION, 3-4 mm apart from each other. The sham-operated groups received only unilateral nerve exposure using the same procedure without ligation.

Behavioral tests and drug application

All behavioral experiments were carried out with the investigators blinded to treatment conditions. Orofacial behavioral tests as described by Vos *et al.* (4) were performed 1 day before and at designated times after CCI-ION surgeries. The rats were placed individually in plastic cages, where they adapted to the testing environments for 2 h. Orofacial response threshold of mechanical sensitivity was determined with a graded series of *von* Frey filaments with bending forces ranging from 0.008 g to 15 g (Ugo Basile, Italy) as described previously

(5-8). The upper limit was set as 15 g filament because the head of rat is turned at this bending force. Stimuli were gently applied to the skin within the infraorbital nerve territory, near the center of the vibrissal pad. Each stimulation consisted of three consecutive applications of the stimulus filament that is 2 s apart. The stimulation is expected to result in behavior responses of head withdrawal and/or escape in rats as defined by Vos *et al* (4). A head withdrawal reaction is typically followed by continuous face wash strokes (at least 3 times) to the stimulated area. An escape reaction is defined as rats moving away from the stimulus filament or attacking the filament. For each session, the complete series of *von* Frey filaments was applied with an increasing force, until the head withdrawal or escape response was triggered. The minimal force applied that triggers such behavior is recorded as the mechanical response threshold. Intra-TG injections were performed with a 28-gauge needle inserted through the infraorbital foramen, infraorbital canal and foramen rotundum. Z941 was a gift from Dr. Terrance Snutch (University of British Columbia). The tip of the needle terminated at the medial part of the TG, 3 μl of the reagent was slowly delivered over a 5 min period, and the needle remained in position 10 min after injection. 5'-Cholesteryl-modified and 2'-O-methyl-modified small interfering RNA (siRNA) for Cav3.2 (Cav3.2-siRNA), agomir-32-5p, antagomir-32-5p, or relevant scrambled controls (RiboBio Biological Technology), labeled with 6-FAM, were diluted to a concentration of 50 μM in DEPC-H_2O. Neuron promoter-specific (human synapsin 1 gene promoter, hSyn) combinatorial lentiviral vectors including lenti-hSyn-miR-32-5p-up (miR-32-up), lenti-hSyn-miR-32-5p-down (miR-32-down), and relevant negative controls (miR-32-NC) containing enhanced green fluorescent protein (EGFP) were obtained from GeneChem (Shanghai). The viral titer was above 1×10^8 TU.

Western blot analysis

Western blot analysis was performed as described previously (7, 9). Briefly, samples containing 20 μg of protein were loaded and separated by 10% (for the Cav3.1, Cav3.2, Cav3.3 and GR proteins) or 12.5% (for the H3K9me2 and H3K27me3 proteins) SDS-polyacrylamide gel electrophoresis and then transferred to polyvinylidene difluoride membranes (Bio-Rad). After blocking with 5% skimmed milk for 1 h, the membranes were incubated overnight at 4 °C

with primary antibodies against the following: Cav3.1 (rabbit, 1:1000, Alomone Labs), Cav3.2 (rabbit, 1:1000, Alomone Labs), Cav3.3 (rabbit, 1:1000, Alomone Labs), GR (rabbit, 1: 1000, Abcam), H3K9me2 (mouse, 1:1000, Abcam), H3K27me3 (mouse, 1:1000, Abcam), H3 (rabbit, 1:1000, Abcam) and GAPDH (rabbit, 1:5000, Abcam). After the primary antibody had been removed, the membrane was washed three times with TBST, followed by incubation with horseradish peroxidase-conjugated goat anti-rabbit (1:8000, R&D Systems) or goat anti-mouse secondary antibody (1:8000, R&D Systems) for 1 h at room temperature. The protein bands were detected with SuperSignal West Pico chemiluminescent substrate (Pierce). Images were captured using the ChemiDoc XRS system and analyzed with Quantity One software (Bio-Rad Laboratories). GAPDH and H3 were used as loading controls to normalize the amounts of proteins.

Real-time quantitative PCR

Total RNA was extracted from the TG tissues using RNAiso Plus (Takara, Japan). According to the protocol provided by the manufacturer of the Hairpin-it^{TM} MicroRNA Quantitation PCR kit (GenePharma), 1 μg of RNA was reverse transcribed to cDNA using a mature hairpin primer specific for miR-32-5p with the following protocol: 16 °C for 30 min, 42 °C for 45 min and 85 °C for 10 min. Real-time PCR was carried out using the ABI 7500 system with the SYBR Green PCR mix (GenePharma) with the following protocol: 94 °C for 3 min, followed by 40 cycles of 94 °C for 15 s and 62 °C for 40 s. All reactions were run in triplicate. U6 was used as an internal control. The relative amount of miR-32-5p in each sample was first normalized to the level of U6 and then normalized to the miR-32-5p expression level in control groups. Relative quantification was performed using the comparative CT ($2^{\wedge-\Delta\Delta}$CT) method. Agarose gel electrophoresis and melting-curve analysis were used to verify the specificity of the amplified PCR product.

Immunofluorescence staining

Immunostaining was conducted as described previously (7, 9, 10). Briefly, TGs were dissected, postfixed in 4% PFA for 4 h, and then cryoprotected in 15~30% sucrose in PB at 4 °C for more than 24 h. Tissue samples were sectioned (15 μm thickness) using a cryostat (CM1950, Leica

Microsystems). Subsequently, the tissue sections were treated with 0.15% Triton X-100 for 30 min and blocked with 5% normal goat serum for 1 h. After overnight incubation at 4 °C with primary antibodies against Cav3.1 (rabbit, 1:500, Alomone Labs), Cav3.2 (rabbit, 1:500, Alomone Labs), Cav3.3 (rabbit, 1:500, Alomone Labs), CGRP (mouse, 1:1000; Abcam), NF-200 (mouse, 1:500, Abcam), H3K9me2 (mouse, 1:500, Abcam) or H3K27me3 (mouse, 1:500, Abcam), the sections were visualized with IB_4-fluorescein isothiocyanate (5 μg/ml; Sigma-Aldrich), Alexa Fluor 555-conjugated goat anti-rabbit IgG (1: 300) or DyLight 488-conjugated goat anti-mouse IgG (1:200) for 2 h at room temperature. After the sections had been washed three times with PBS at room temperature, images were captured under an upright fluorescence microscope (Nikon 104C) with a CoolSnap HQ2 CCD camera (Photometrics).

Fluorescence *in situ* Hybridization

LNA-digoxin-labeled probes specific for miRNA-32-5p and negative control probes were obtained from Exon. In brief, animals were fixed via the ascending aorta with PBS containing 4% paraformaldehyde and 0.1% DEPC. TG samples were sectioned using a cryostat (CM1950, Leica Microsystems). The sections were then washed 3 times with DEPC-PBS and incubated for 10 min in acetylation buffer (containing triethanolamine, HCl, and acetic anhydride in DEPC-H_2O). After rinsing 3 times in DEPC-PBS, the sections were prehybridized in miRNA hybridization buffer (containing formamide, dextran sulfate, saline-sodium citrate, Denhardt's solution and yeast RNA) at 55 °C for 2 h. The probe miR-32-5p (rno-miR-32-5p miRCURY LNA detection probe, 5'-digoxin-TGCAACTTAGTAATGTGCAATA–digoxin-3') or a negative control probe was denatured at 85 °C for 3 min in miRNA hybridization buffer (at a final 50 nM concentration) and stabilized at 4 °C for 2 min. For hybridization, sections were incubated with the denatured hybridization probe for 36 h at 40 °C. After hybridization, the sections were rinsed in washing buffer (containing formamide and saline-sodium citrate) three times and blocked for 1 h in blocking buffer at 37 °C, followed by incubation in Cy3-labeled anti-digoxin antibody (diluted in blocking buffer at 1:150) for 1 h. For co-labeling experiments, the sections were first hybridized with the probe of miRNA-32-5p, then co-incubated with rabbit anti-Cav3.2 (1:300, Alomone Labs), mouse anti-H3K9me2 (1:500, Abcam), mouse anti-

H3K27me3 (1:500, Abcam), and rabbit anti-GR (1:300, Cell Signaling Technology), respectively, overnight at 4 °C. The fluorescent signals were developed with appropriate fluorescence conjugated secondary antibodies including DyLight 488-conjugated goat anti-rabbit IgG (1:300, Cell Signaling Technology) or DyLight 488-conjugated goat anti-mouse IgG (1:300, Cell Signaling Technology). The sections were finally mounted using glycerinum or 4',6-diamidino-2-phenylindole (DAPI)-antifade Solution (Guangzhou Exon Technology). After incubation in DEPC-PBS, the sections were mounted, observed and photographed under a fluorescence microscope.

Luciferase reporter assay

Prediction of miRNA targets was carried out with the databases TargetScan (www.targetscan.org/) and miRDB (www.mirdb.org/). The mRNA for the full-length 3'-UTR of Cav3.2 was amplified by PCR from rat cDNA. The following specific primers were used: wild-type forward 5'-CCGCTCGAGGCGTGTCCACAGGGCTTTG-3', wild-type reverse 5'-TCCGAAGATCTCAGATTTGCCTTGCCCCTCC-3'; mutant forward 5'-CGTGGTACC GCATCTGATGCAGAAAACTTGGCTTCC-3', and mutant reverse 5'-GGCCAAGTCCT TTGTAGAAACGGATGACATAAAGCAAA-3'. Plasmids encoding firefly luciferase followed by the wild-type Cav3.2 3'-UTR (Cav3.2-wt) or mutant Cav3.2 3'-UTR (Cav3.2-mut) were constructed (Genomeditech). Cav3.2-wt and Cav3.2-mut were inserted into the pGL3 plasmid downstream of the luciferase gene. The binding sites for the transcription factors NF1, C/EBPβ and GR within the 148 bp sequence of the miR-32-5p gene promoter region were predicted with the databases AliBaba2.1 (http://gene-regulation.com) and PROMO (http://alggen.lsi.upc.es). The full-length 148 bp fragments from the miR-32-5p gene promotor region (miR-32-5p-wt) were also individually cloned into the pGL3 plasmid encoding firefly luciferase. In addition, sequences of the miR-32-5p promotor region with mutant binding sites for NF-1 (mut-NF-1), C/EBPβ (mut-C/EBPβ) or GR (mut-GR) were constructed and inserted into the pGL3 plasmid. All the constructs were generated by GeneWiz (Suzhou). pGMR-TK containing Renilla luciferase was cotransfected with pGL3 for data normalization. The constructed vector was confirmed by DNA sequencing. After HEK293T cells were seeded at 1

$\times 10^5$ cells in 24-well plates, the Cav3.2-wt-3'-UTR or Cav3.2-mut-3'-UTR plasmid (50 ng), pGMR-TK (10 ng) and miR-32-5p mimics (100 ng) (or the negative control) were transfected into HEK293T cells using Lipofectamine 2000^{TM} (Invitrogen). Similarly, miRNA32-wt (500 ng), mut-NF-1 (500 ng), mut-C/EBPβ (500 ng), mut-GR (500 ng), and pGMR-TK (100 ng) were transfected into PC12 cells using Lipofectamine 2000^{TM} (Invitrogen). Forty-eight hours after transfection, a Dual-Glo luciferase assay system (Promega) was used to measure the firefly and Renilla luciferase activities. First, firefly luminescence activity was measured following Dual-Glo luciferase reagent treatment. Then, Dual-Glo Stop and Glo reagent was added to each well, and the Renilla luciferase activity was assayed. Firefly luminescence activity was divided by Renilla luciferase activity.

Chromatin immunoprecipitation-PCR

ChIP was performed using a SimpleChIP® plus Enzymatic Chromatin IP kit (Cell Signaling Technology) according to the manufacturer's protocol. Briefly, TGs from sham-operated and CCI-ION rats were finely minced in PBS containing a protease inhibitor cocktail. To crosslink the proteins and DNA, TG lysates were incubated in 1.5% formaldehyde for 20 min, and glycine was used to stop the crosslinking reaction. To obtain cell suspensions, tissues were disaggregated with a tissue homogenizer. To obtain DNA fragments with lengths of approximately 150-900 bp, nuclear tissues were digested using micrococcal nuclease for 20 min at 37 °C and sonicated in ChIP buffer, and 0.5 M EDTA was used to stop digestion. The sonicated samples were centrifuged at 9,400 *rpm* for 10 min at 4 °C. Two percent of the supernatant was used as a DNA input control, and the remaining samples were incubated with 5 μl of IgG (negative control, Cell Signaling Technology), H3K9me2 (Abcam), H3K27me3 (Abcam) or GR (Cell Signaling Technology) and rotated at 4 °C overnight to pull down chromatin. Immunoprecipitated complexes were collected using ChIP-grade protein G magnetic beads (Cell Signaling Technology) and then washed three times with low-salt immune complex wash buffer and once with high-salt immune complex wash buffer. The bound proteins were eluted with ChIP elution buffer containing 1% SDS and 0.1 M $NaHCO_3$. Crosslinking of protein-DNA complexes was reversed with incubation with proteinase K at 65 °C for 2 h, and

DNA was purified using DNA purification columns. ChIP-enriched DNA was analyzed by qPCR using the following ChIP primers (forward 5'-CTTTTCTCCTCACT CCTGCTCA-3' and reverse 5'-ACACTCCCAACCTGGAATCTTT-3'. Enrichment of the miR-32-5p promoter was assessed relative to normalized values obtained with the same input sample. The PCR product was separated by 2% agarose gel electrophoresis.

Dissociation of TG neurons

TG neurons were dissociated as described in our previous studies (7). Briefly, TGs dissected from Sprague-Dawley rats (140-160 g, male) were treated with 4.5 mg/ml collagenase D (Roche) for 50 minutes and 2.5 mg/ml trypsin (Sigma) for 10 min in DMEM saturated with mixed CO_2/O_2 gas at 37 °C. After the enzymatic digestion was stopped by washing three times in PBS, the ganglia were resuspended in neurobasal medium (Gibco) (supplemented with 2 mM L-glutamine and 2% B27). Sterilized Pasteur pipettes (Fisher Scientific) with fire-polished tips were used to separate the neurons with gentle trituration. After centrifugation, the TG neurons were resuspended and transferred onto Matrigel (BD Biosciences)-coated coverslips. Electrophysiology was conducted between 3 and 6 hours after plating.

Electrophysiology

Whole-cell patch clamp recordings were carried out at room temperature (22-24 °C) as described in our previous studies (7, 9). In brief, recording electrodes pulled from 1.5-mm borosilicate glass capillaries (Warner Instruments) with a micropipette puller (P-97, Sutter Instruments) had resistance of 3-4 MΩ when filled with an internal solution containing (in mM) 110 CsCl, 0.3 Na_2-GTP, 4 Mg-ATP, 10 EGTA, and 25 HEPES with a pH adjusted to 7.4 with CsOH and an osmolarity of 295 mOsm. Neurons were tested in an external solution containing (in mM): 140 TEA-Cl, 5 $BaCl_2$, 0.5 $MgCl_2$, 5 CsCl, 10 HEPES, and 5.5 D-glucose with a pH adjusted to 7.3 with TEA-OH and an osmolarity of 305 mOsm. We recorded Ba^{2+} currents at -40 mV for 40 ms by depolarizing step pulse from either -60 mV or -110 mV holding potential after the addition of 5 μM nifedipine (L-type channel blocker), 0.2 μM ω-conotoxin MVIIC (both N- and P/Q-type channel blocker), and 0.2 μM SNX-482 (R-type channel blocker) to the external solution. Currents through T-type channels were then calculated by digitally

subtracting current measured from -60 mV from those measured from -110 mV. This eliminated the residual HVA currents that were not blocked by the blockers (11, 12). Unless otherwise indicated, compounds were puff-applied with an air pressure microinjector (Pneumatic PicoPump PV820, World Precision Instruments). Retrograde tracing of neurons innervating the skin of the whisker pad was performed by subcutaneous injection of (DiI, 20 mg/ml, Invitrogen) into the center of the left cushion using a 25-μl Hamilton microsyringe fitted with a 28-gauge needle. Four days after injection, small TG neurons were subjected to patch clamp recording. In the present study, we sorted adult rat TG neurons into small (soma diameter < 30 μm) and medium (soma diameter 30-45 μm) neurons and conducted electrophysiological recordings in small neurons, which are primarily nociceptors (7, 13).

Data analysis and statistics

Values are reported as the mean ± SEM. Data acquisition and statistical analysis were performed using ClampFit 10.2 (Molecular Devices), Prism 6.0 (GraphPad Software), and Microsoft Excel. Plots showing voltage-dependent activation and steady-state inactivation were fitted by the Boltzmann equation. Statistical comparisons of several groups were performed using one-way analysis of variance (ANOVA) and subsequent Bonferroni correction if not stated otherwise. The paired or unpaired *t*-test was used to compare two groups as appropriate. The behavioral data were analyzed by two-way repeated-measures ANOVA with a *post hoc* Bonferroni test. Differences with $p < 0.05$ were considered to be statistically significant.

SI References

1. G. J. Bennett, Y. K. Xie, A peripheral mononeuropathy in rat that produces disorders of pain sensation like those seen in man. *Pain* **33**, 87-107 (1988).
2. Y. B. Martin, C. Avendano, Effects of removal of dietary polyunsaturated fatty acids on plasma extravasation and mechanical allodynia in a trigeminal neuropathic pain model. *Mol Pain* **5**, 8 (2009).
3. D. Christensen, M. Gautron, G. Guilbaud, V. Kayser, Combined systemic administration of the glycine/NMDA receptor antagonist, (+)-HA966 and morphine attenuates pain-related behaviour in a rat model of trigeminal neuropathic pain. *Pain*

83, 433-440 (1999).

4. B. P. Vos, A. M. Strassman, R. J. Maciewicz, Behavioral evidence of trigeminal neuropathic pain following chronic constriction injury to the rat's infraorbital nerve. *J Neurosci* **14**, 2708-2723 (1994).
5. W. J. Dixon, Efficient analysis of experimental observations. *Annu Rev Pharmacol Toxicol* **20**, 441-462 (1980).
6. K. W. Li *et al.*, Calcium channel alpha2delta1 proteins mediate trigeminal neuropathic pain states associated with aberrant excitatory synaptogenesis. *J Biol Chem* **289**, 7025-7037 (2014).
7. H. Wang *et al.*, Brain-derived neurotrophic factor stimulation of T-type Ca(2+) channels in sensory neurons contributes to increased peripheral pain sensitivity. *Sci Signal* **12**, eaaw2300 (2019).
8. V. Kayser, B. Aubel, M. Hamon, S. Bourgoin, The antimigraine 5-HT 1B/1D receptor agonists, sumatriptan, zolmitriptan and dihydroergotamine, attenuate pain-related behaviour in a rat model of trigeminal neuropathic pain. *Br J Pharmacol* **137**, 1287-1297 (2002).
9. Y. Zhang *et al.*, Peripheral pain is enhanced by insulin-like growth factor 1 through a G protein-mediated stimulation of T-type calcium channels. *Sci Signal* **7**, ra94 (2014).
10. Y. Zhang *et al.*, Neuromedin B receptor stimulation of Cav3.2 T-type Ca(2+) channels in primary sensory neurons mediates peripheral pain hypersensitivity. *Theranostics* **11**, 9342-9357 (2021).
11. J. Tao *et al.*, Effects of familial hemiplegic migraine type 1 mutation T666M on voltage-gated calcium channel activities in trigeminal ganglion neurons. *J Neurophysiol* **107**, 1666-1680 (2012).
12. Y. Zhang, M. Mori, D. L. Burgess, J. L. Noebels, Mutations in high-voltage-activated calcium channel genes stimulate low-voltage-activated currents in mouse thalamic relay neurons. *J Neurosci* **22**, 6362-6371 (2002).
13. Y. Zhang *et al.*, Melatonin-mediated inhibition of Cav3.2 T-type Ca(2+) channels induces sensory neuronal hypoexcitability through the novel protein kinase C-eta isoform. *J Pineal Res* **64**, e12476 (2018).

SI Figures S1 to S16

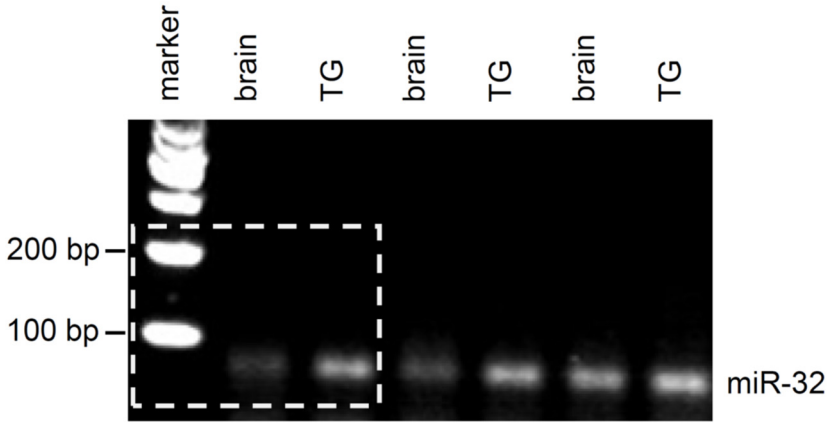

Fig. S1: RT-PCR analysis of miR-32 in the brain and TGs of naïve rats. Shown is the expanded image of RT-PCR for miR-32 presented in Fig. 1D.

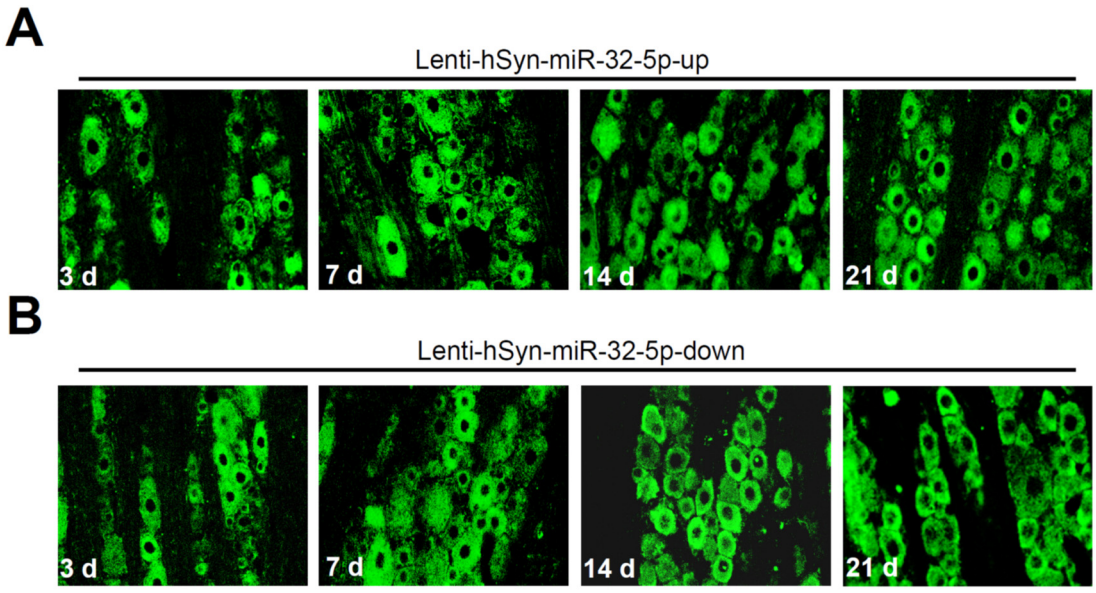

Fig. S2: Validation of lentiviral delivery in naive TGs. The expression of lenti-hSyn-miR-32-5p-up (miR-32-up, *A*) or lenti-hSyn-miR-32-5p-down (miR-32-down, *B*) carrying the construct encoding EGFP was observed in various sized TG neurons at 3 days after intra-TG injection, and was maintained on day 21.

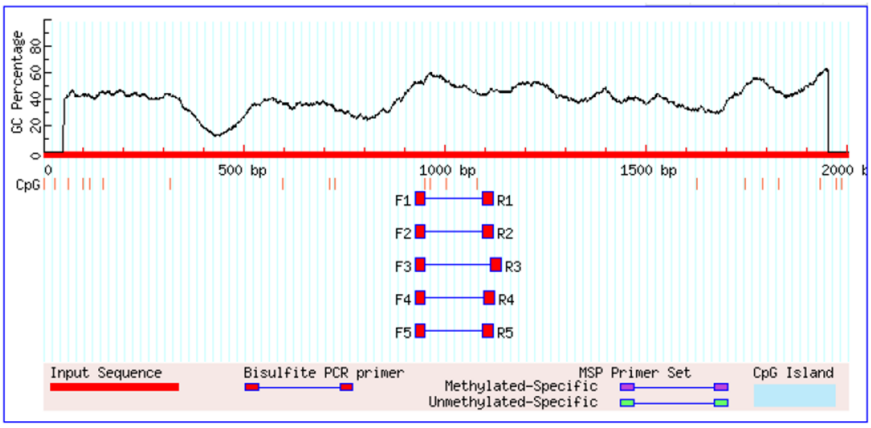

Sequence Name:
Sequence Length: 2001

CpG island prediction results
(Criteria used: Island size > 100, GC Percent > 50.0, Obs/Exp > 0.6)
No CpG islands were found in your sequence
Primer picking results for bisulfite sequencing (or restriction) PCR

Fig. S3: Bioinformatics prediction by MethPrimer suggested that no CpG islands were found in miR-32 promoter region.

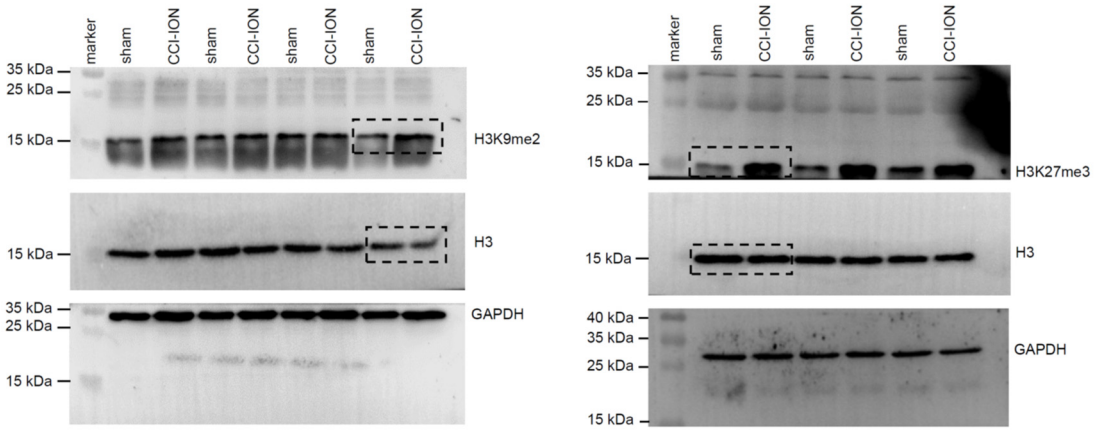

Fig. S4: Immunoblots showing the protein expression levels of H3K9me2 and H3K27me3 in rat TGs. Shown are the expanded images of Western blots presented in Fig. 3A. Blots are representative of three experiments.

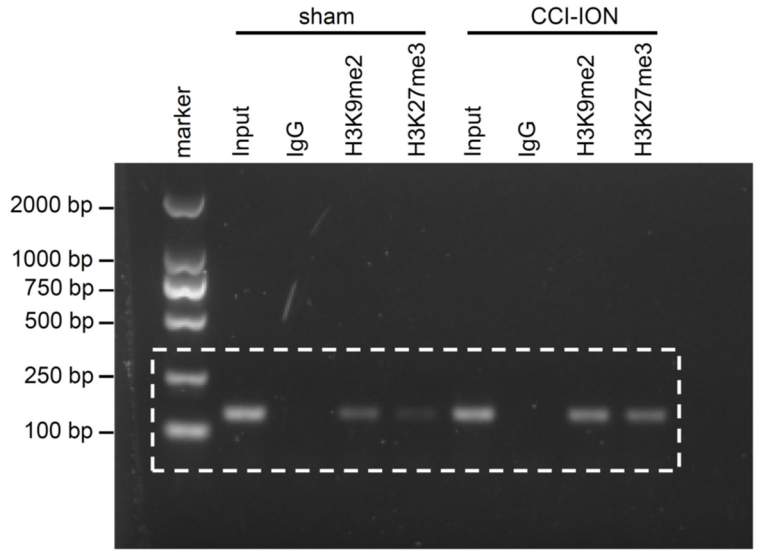

Fig. S5: Blots of ChIP-qPCR analysis show that the binding activity of H3K9me2 or H3K27me3. Shown is the expanded image presented in Fig. 3D.

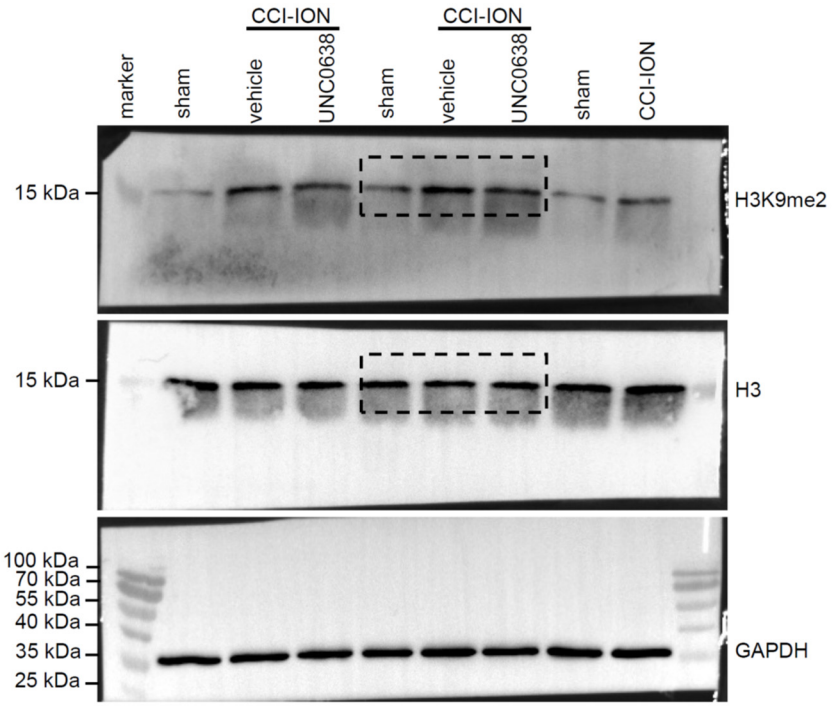

Fig. S6: Intra-TG injection of UNC0638 (5 nmol) attenuated the increased expression of H3K9me2 in the ipsilateral TGs on day 14 post-CCI-ION. Shown are the expanded images respectively presented in Fig. 3F. Blots are representative of three experiments.

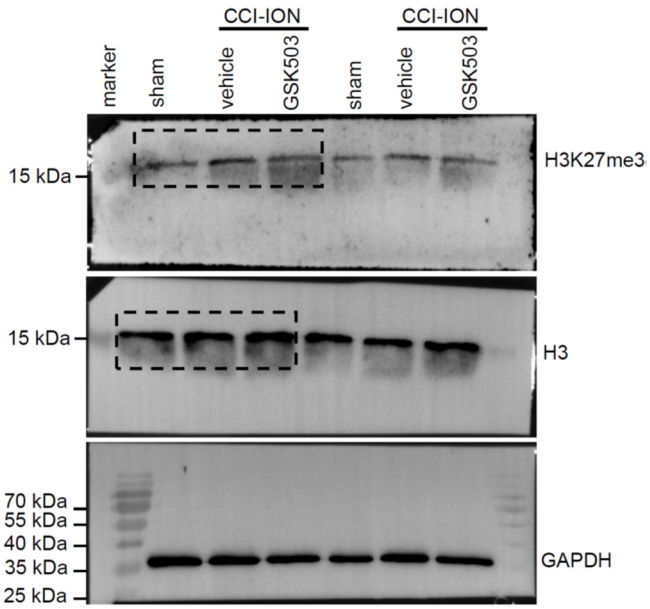

Fig. S7: Intra-TG injection of GSK503 (5 nmol) attenuated the increased expression of H3K27me3 in the ipsilateral TGs on day 14 post-CCI-ION. Shown are the expanded images respectively presented in Fig. 3G. Blots are representative of three experiments.

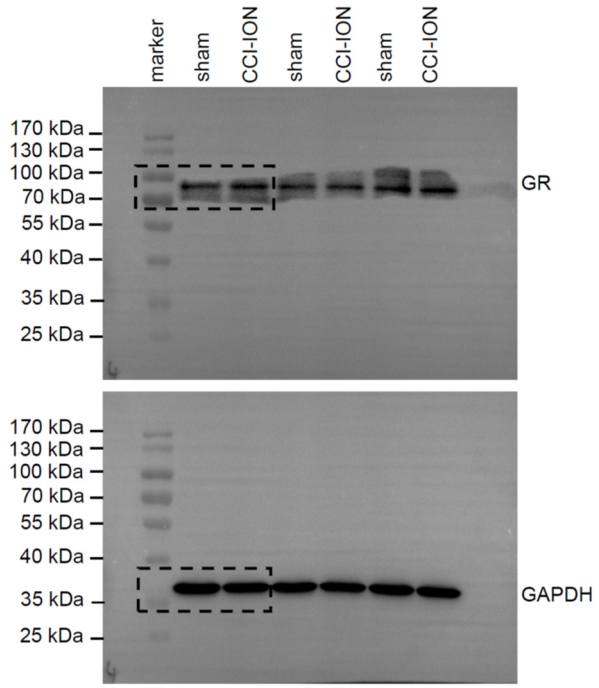

Fig. S8: Protein expression of GR in rat TGs after peripheral nerve injury. Shown is the expanded image of Western blot for GR against a loading control, GAPDH, respectively presented in Fig. 4E. Blots are representative of three experiments.

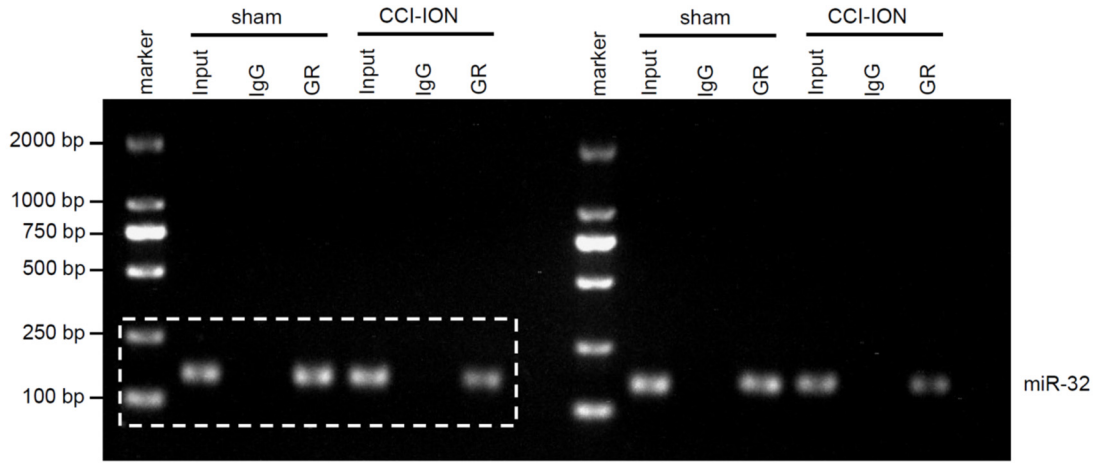

Fig. S9: Blots of ChIP-PCR showing the expression levels of GR at the promoter region of miR-32 in TGs. Shown is the expanded image presented in Fig. 4F.

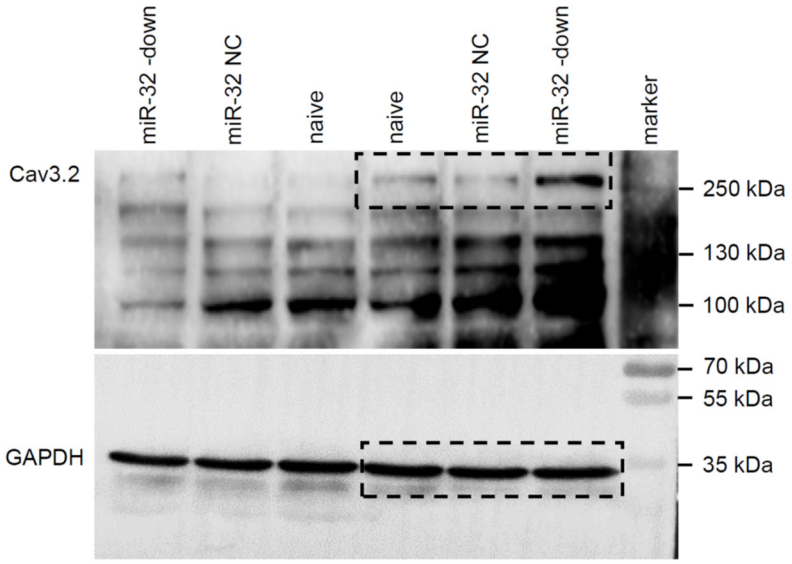

Fig. S10: Intra-TG injection of miR-32-down increased the protein expression of Cav3.2 in naïve rats. Shown is the expanded image of Western blot for Cav3.2 against a loading control, GAPDH, presented in Fig. 5F. Blots are representative of three experiments.

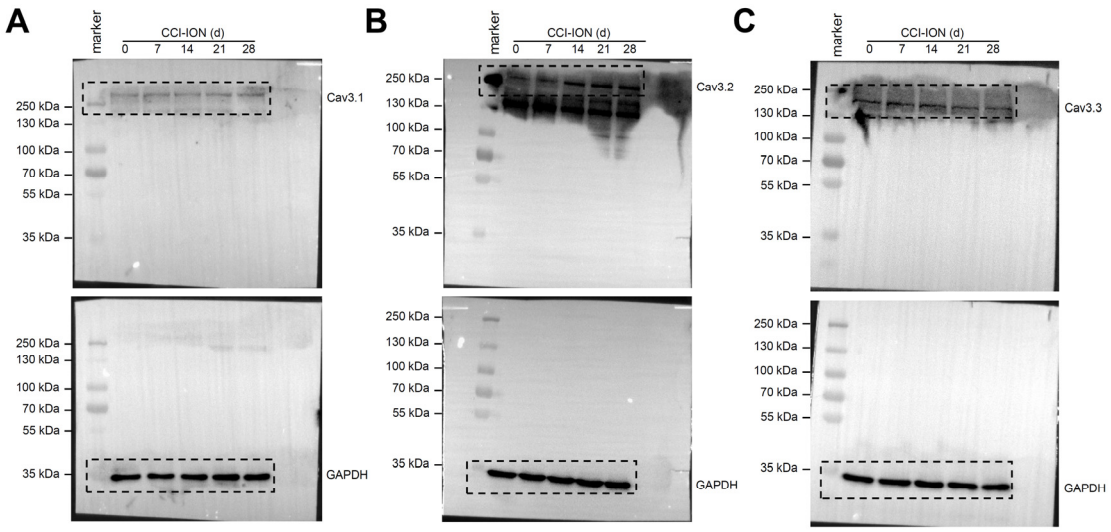

Fig. S11: Upregulation of Cav3.2 in rat TGs after peripheral nerve injury. Shown is the expanded image of Western blot for Cav3.1 (*A*), Cav3.2 (*B*) and Cav3.3 (*C*) against a loading control, GAPDH, respectively presented in Figs. 6A-C. Blots are representative of three experiments.

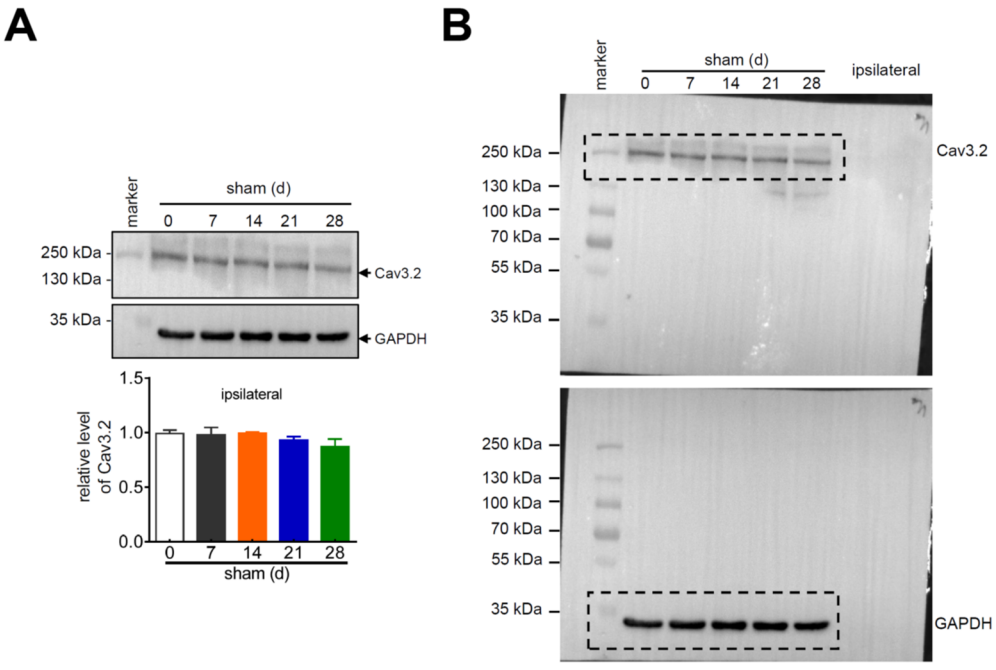

Fig. S12: A, the sham operation did not alter the basal expression of Cav3.2 proteins in the ipsilateral TGs following surgery. **B,** the expanded image of Western blot for Cav3.2 against a loading control, GAPDH, presented in panel *A*. Blots are representative of three experiments.

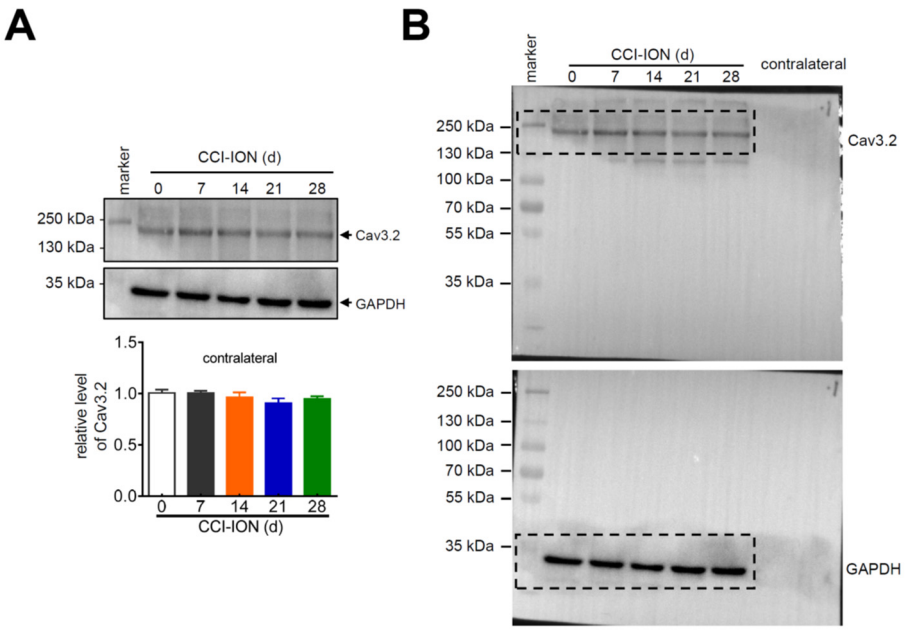

Fig. S13: A, the basal expression of Cav3.2 proteins in the contralateral TGs remained unchanged in CCI-ION 14 d rats. **B,** the expanded image of Western blot for Cav3.2 against a loading control, GAPDH, presented in panel *A*. Blots are representative of three experiments.

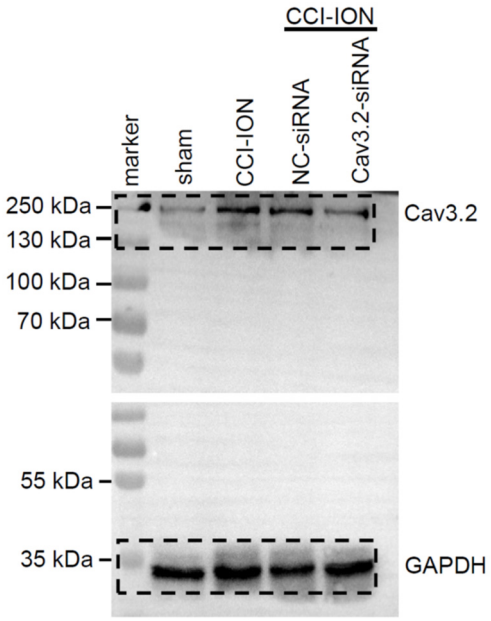

Fig. S14: The increased expression level of Cav3.2 induced by CCI-ION was attenuated by intra-TG injection of Cav3.2-siRNA. Shown is the expanded image of Western blot for Cav3.2 against a loading control, GAPDH, presented in Fig. 6L. Blots are representative of three experiments.

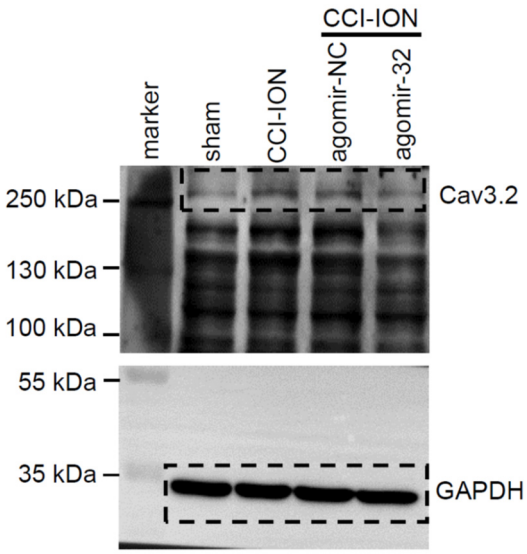

Fig. S15: The increased expression level of Cav3.2 induced by CCI-ION was attenuated by intra-TG injection of agomir-32. Shown is the expanded image of Western blot for Cav3.2 against a loading control, GAPDH, presented in Fig. 7A. Blots are representative of three experiments.

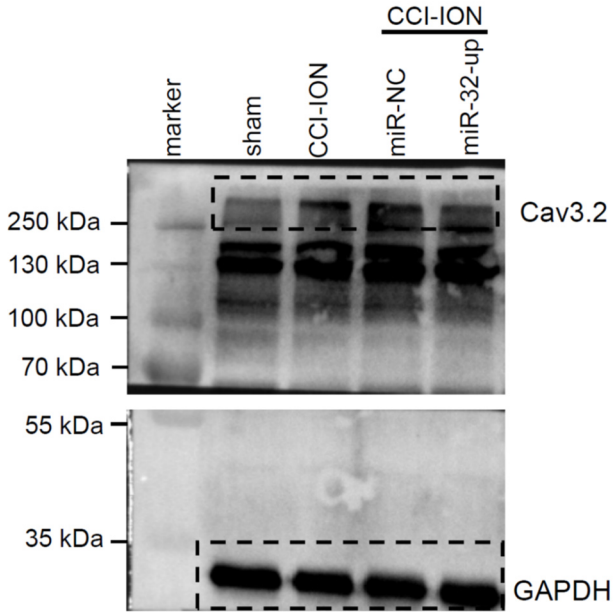

Fig. S16: The increased expression level of Cav3.2 induced by CCI-ION was attenuated by intra-TG injection of miR-32-up. Shown is the expanded image of Western blot for Cav3.2 against a loading control, GAPDH, presented in Fig. 7E. Blots are representative of three experiments.